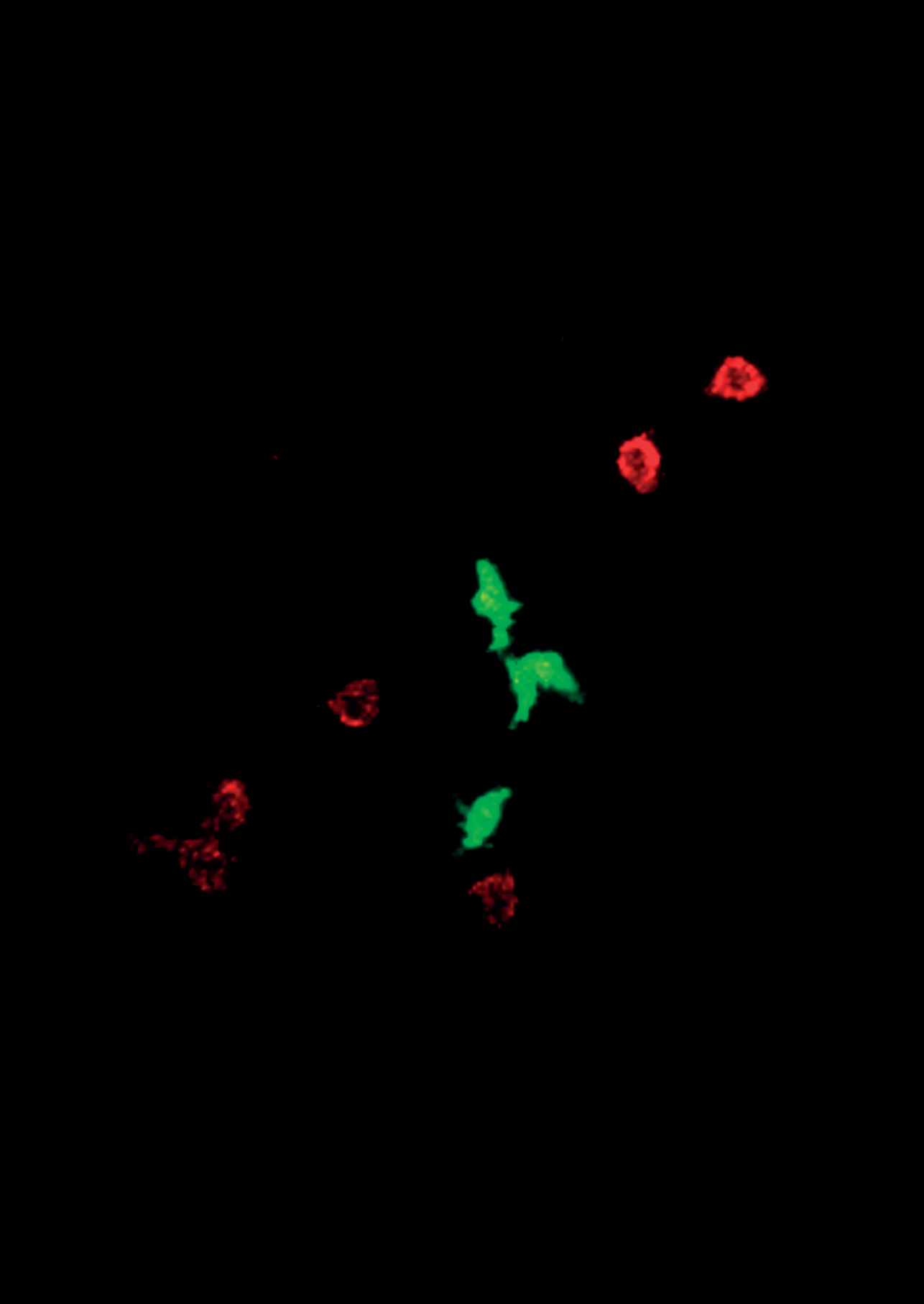

Chapter 6

Skin-resident memory CD8$^+$ T cells trigger a state of tissue-wide pathogen alert

Silvia Ariotti[1], Marc A Hogenbirk[2,*], Feline E Dijkgraaf[1,*], Lindy L Visser[1], Mirjam E Hoekstra[1], Ji-Ying Song[3], Heinz Jacobs[2], John B Haanen[1] and Ton N Schumacher[1,#]

Science, 2014, Oct, 3;346(6205):101-5. doi: 10.1126/science.1254803

[1] Division of Immunology, Netherlands Cancer Institute, Amsterdam, Netherlands.

[2] Division of Biological Stress Response, Netherlands Cancer Institute, Amsterdam, Netherlands.

[3] Experimental Animal Pathology, Netherlands Cancer Institute, Amsterdam, Netherlands.

* These authors contributed equally to this work

To whom correspondence should be addressed: t.schumacher@nki.nl

ABSTRACT

After an infection, pathogen-specific tissue-resident memory T cells (T_{RM} cells) persist in non-lymphoid tissues to provide rapid control upon reinfection, and vaccination strategies that create T_{RM} cell pools at sites of pathogen entry are therefore attractive. However, it is not well understood how T_{RM} cells provide such pathogen protection. Here, we demonstrate that activated T_{RM} cells in mouse skin profoundly alter the local tissue environment by inducing a number of broadly active antiviral and antibacterial genes. This “pathogen alert” allows skin T_{RM} cells to protect against an antigenically unrelated virus. These data describe a mechanism by which tissue-resident memory $CD8^+$ T cells protect previously infected sites that is rapid, amplifies the activation of a small number of cells into an organ-wide response, and has the capacity to control escape variants.

RESULTS

Tissue-resident memory $CD8^+$ T cells (T_{RM} cells) are a subtype of memory lymphocytes (1) that permanently reside in non-lymphoid tissues in mice and humans (2–11). Analysis of herpes simplex virus (HSV)–1 and HSV-2 shedding episodes in infected human mucosa has shown that emerging lesions are often controlled within 6 to 12 hours (12). Furthermore, the severity of viral lesions during reactivation is likely determined by local immune control, and data in mouse models suggest that such tissue protection can be mediated by locally residing memory $CD8^+$ T cells (13–15).

The mechanisms by which a small number of local memory cells can protect a peripheral tissue have not been established and, given the low numbers of T_{RM} cells in tissues, unlikely to solely involve the direct killing of target cells (16). In addition, although T_{RM} cells are able to recruit circulating memory $CD8^+$ T cells to the peripheral tissue within 48 hours of activation (17), such recruitment is unlikely to achieve early pathogen control (12).

To investigate how small numbers of tissue resident memory T cells confer rapid protection of local tissue, we created a pool of T_{RM} cells by intra-epidermal DNA vaccination of mice that had received small numbers of green fluorescent protein CD8 T cells specific for the HSV-1–derived glycoprotein B peptide ($gB_{498-505}$ (gBT-GFP hereafter)) (**fig. S1**) (9, 18). Weeks later, skin areas harboring T_{RM} cells were challenged with HSV-1 or $gB_{498-505}$ peptide. Immunohistochemical analysis of HSV-1–infected or $gB_{498-505}$ peptide–challenged skin tissue of gBT-GFP T_{RM} cell mice and naive mice at 9 hours after infection/peptide administration did not reveal any difference in the infiltration of macrophages, gBT-GFP memory T cells, or CD3 cells. A moderate increase in the number of neutrophils was only observed upon peptide administration (**fig. S2, A-F**). To evaluate other possible effects of T_{RM} cell activation on the surrounding tissue, we obtained transcriptional profiles from the entire skin tissue at the same early time point after *in situ* triggering of T_{RM} cells. Comparison of the transcriptional profiles in skin exposed to control [ovalbumin ($OVA_{257-264}$)] peptide or cognate ($gB_{498-505}$) peptide revealed differential expression of a large number of genes [cut-offs: false discover rate (FDR) < 0.05; log2 fold change > T 1.2] (**Fig. 1A** and **fig. S3**). To distinguish between noise caused by variation in tissue composition and signal due to T_{RM} cell triggering, transcriptional profiling was performed on a second cohort of mice (**Fig. 1B** and **fig. S3**). Genes the expression of which was altered at a comparable magnitude in both data sets (difference in magnitude of induction <1.5; blue in **fig. S3B**) were retained for further analysis.

To determine whether the observed changes in gene expression were due to T cell receptor (TCR) recognition of antigen, cohorts of mice harboring T_{RM} cells specific for the $OVA_{257-264}$ epitope (OTI hereafter) were challenged with either $gB_{498-505}$ or $OVA_{257-264}$ antigen. In this setup, activation of the OTI-GFP T_{RM} cells by cognate $OVA_{257-264}$ resulted in a reproducible change of the skin transcriptional profile (**Fig. 1, C** and **D**). Furthermore, changes in gene expression in gBT-GFP skin T_{RM} cells challenged with cognate $gB_{498-505}$ peptide

and OTI-GFP T_{RM} cells challenged with cognate $OVA_{257-264}$ peptide were highly correlated (**Fig. 1E**). Thus, triggering of T_{RM} cells harboring skin with peptide antigen leads to a rapid alteration in the transcriptome that is visible at the level of the entire tissue before substantial influx of immune cells is seen.

Combination of all four data sets resulted in a list of 89 genes that are differentially expressed (all increased) upon specific triggering of T_{RM} cells (**table S1** and **Fig. 1E**). Induction of part of this gene set was already observed 3 hours after antigen administration, and induction was essentially complete after 6 hours (**fig. S4**). Supporting the immunohistochemical results, T cell–specific genes did not show any significant difference between T_{RM} cells harboring skin treated with specific or control peptide (**fig. S5**). Independent full transcriptome gene ontology analyses (19) of the four data sets indicated inflammation and immunity as dominant signatures of all data sets (**table S2**).

Transcriptome analysis of two independent experiments in which gBT-GFP T_{RM} cell skin was challenged with HSV-1 or control showed a similar pattern of gene induction. For most genes within the gene set (**table S1**), the magnitude of induction was larger upon peptide triggering, possibly because a greater number of T_{RM} cells can encounter antigen early after peptide administration (group 1 in **Fig. 1F**). In addition, a second group of genes, including a large number of chemokines and cytokines involved in innate immune cell movement, was more strongly or only up-regulated upon virus infection (group 2 in **Fig. 1F**). Together, these data show that antigen specific activation of T_{RM} cells is sufficient to initiate an early response that is visible at the level of the entire tissue.

Strikingly, many of the genes that were induced upon peptide administration were expressed at levels >10 to >100 times the level of T cell–specific genes (**Fig. 1G**). Furthermore, analysis of the identified gene set revealed the induction of a broad-spectrum anti-pathogen response. To dissect whether this rapid tissue response depends upon systemic antigen-specific memory T cells, or only requires the T_{RM} cell population, OTI-GFP cells from male donors were transferred into syngeneic female recipients and activated by vaccination. In this setting, the systemic memory T cell pool (central memory + effector memory cells; T_{CM} + T_{EM})—but not the tissue-resident memory pool—is cleared (5) (**fig. S1**). Comparison of the transcriptional profile in skin of recipients harboring either T_{RM} cells or both T_{RM} and T_{CM} + T_{EM} cells indicates that activation of the T_{RM} cell pool is sufficient to induce expression of the large series of genes within skin (**Fig. 2A**).

Upstream regulator analysis of the induced gene signatures by Ingenuity Pathway Analysis indicated that the cytokine interferon-γ (IFN-γ) is the most likely factor controlling the transcriptional alterations seen in T_{RM} cell–conditioned skin (**table S3**), and previous work has shown that $CD8^+$ T_{RM} cells rapidly re-express IFN-γ after local antigen rechallenge (17). Analysis of full-thickness skin 9 hours after triggering of a population of wild-type or $Ifng^{-/-}$ T_{RM} cells revealed that a large part of the transcriptional alterations seen upon T_{RM} cell triggering are dependent on T_{RM} cell–derived IFN-γ (**Fig. 2B**). Furthermore, this IFN-γ

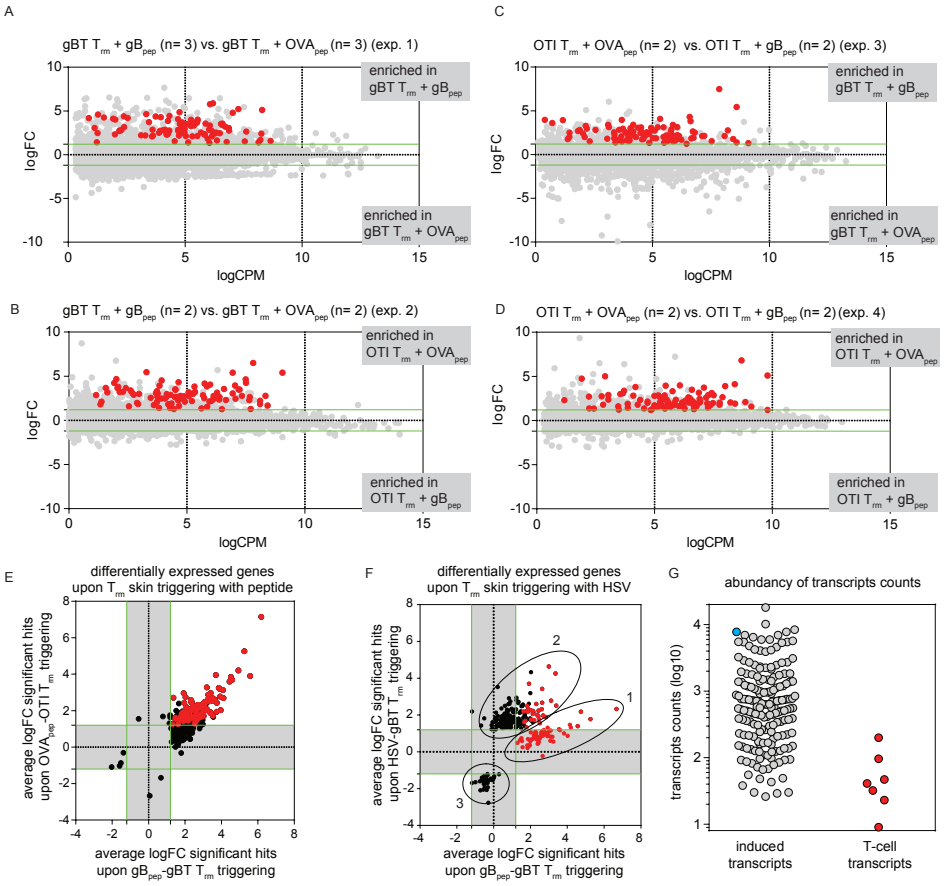

Figure 1 | T_{RM} cell triggering alters tissue-wide gene expression profiles. (**A** to **D**) Transcriptome analysis of full-thickness skin from mice harboring gBT-GFP T_{RM} cells (**A** and **B**) or OTI-GFP T_{RM} cells (**C** and **D**) upon local administration of either $gB_{498-505}$ or $OVA_{257-264}$ peptide. Relative abundance is plotted for averaged normalized read counts. All detected nondifferentially expressed genes are depicted in gray. Genes that are differentially expressed in all four comparisons (log fold change (logFC) > T1.2; FDR < 0.05; difference in magnitude between replicate experiments < 1.5) (fig. S3) are depicted in red. In these and further plots, horizontal green lines represent logFC limits for significance T1.2. (**E**) Average logFC for gBT T_{RM} cells and OTI T_{RM} cells harboring skin upon triggering with cognate peptide. Genes listed in table S1 (differentially expressed upon T_{RM} cell triggering) are shown in red; genes that were only up-regulated in one of the T_{RM} cell groups in black. (**F**) Average logFC for skin harboring gBT T_{RM} cells upon triggering with either HSV-1 or cognate peptide. Genes listed in table S1 are shown in red; genes specifically up-regulated upon HSV-1 infection are depicted in black. Group 1, correlated behavior between both triggers, enriched in interferon-responsive genes; group 2, preferentially or only induced by HSV, enriched in secreted molecules; group 3, reduced by HSV, too small for pathway analysis. (**G**) Comparison of normalized transcript counts of the differentially expressed gene set in table S1 (induced transcripts) with normalized transcript counts of a set of T cell–specific genes (T cell transcripts). Among induced transcripts, IFITM3 is depicted in blue; the T cell transcripts gene set (IFN-γ, CD2, zap70, CD5, CD69, CD8a, and CD8b1) is depicted in red. Values are representative of eight comparisons.

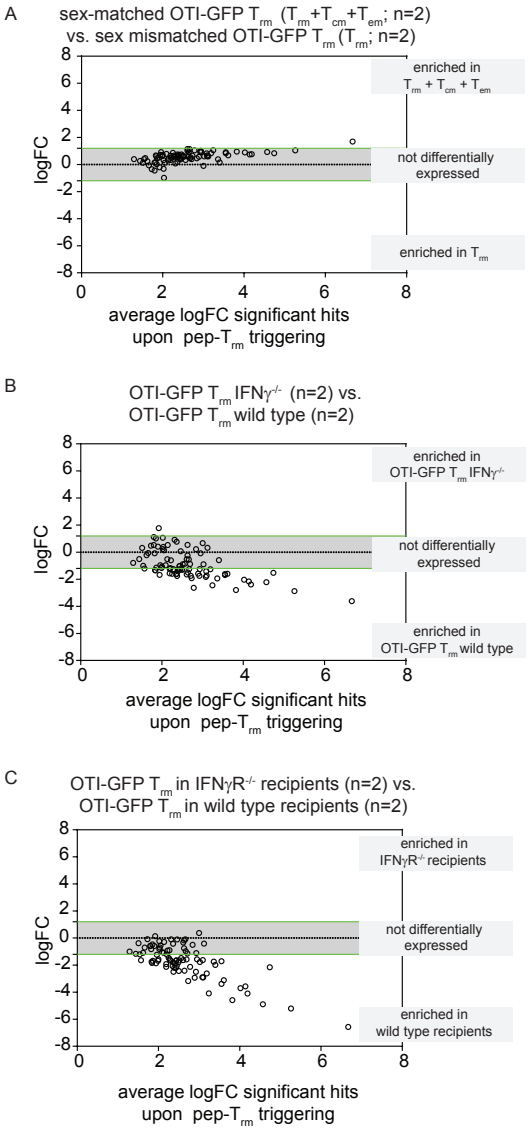

Figure 2 | T_{RM} cells mediate the induction of an antiviral state through IFN-γ. (**A**) Female recipients of either sex-matched or mismatched OTI-GFP$^+$ cells were vaccinated to induce skin T_{RM} cells. Skin areas harboring T_{RM} cells were treated locally with $OVA_{257-264}$ peptide and sacrificed 9 hours later. The absence of systemic memory T cells (see fig. S1) does not significantly reduce tissue conditioning by peptide triggering. On average, induction of the identified gene set was slightly more pronounced in sex-matched recipients (by a factor of 1.15, not significant), which could either reflect a limited contribution of the circulating memory T cell pool or the slight reduction in T_{RM} cell numbers in skin of mismatched recipients (fig. S1F). (**B**) Recipients of OTI-GFP$^+$ T_{RM} cells derived from either wild-type or IFN-γ–deficient donors were vaccinated to induce skin T_{RM} cells, and the effect of T_{RM} cell triggering was then analyzed as in (A). (**C**) IFN-γ receptor–proficient or -deficient recipients of OTI-GFP$^+$ T_{RM} cells were vaccinated to induce skin T_{RM} cells, and the effect of T_{RM} cell triggering was then analyzed as in (A).

acts on skin cells other than T_{RM} cells themselves, as the tissue response is also largely lost in Ifngr1$^{-/-}$ recipient mice in which only T_{RM} cells express IFN-γ receptor 1 (**Fig. 2C**). These data suggest that shortly after TCR triggering, activated T_{RM} cells express IFN-γ to enhance expression of proteins involved in pathogen control within the surrounding tissue. To test this hypothesis, we analyzed the expression pattern of IFITM3 (interferon-induced transmembrane protein 3; blue in **Fig. 1G**), a protein with broad-spectrum antiviral activity (20), and one of the transcripts induced by T_{RM} cell triggering (**Fig. 1** and **table S1**). Within 6 hours of T_{RM} cell activation by cognate antigen, most epidermal and dermal cells expressed IFITM3, with maximal levels at 9 to 18 hours after conditioning (**Fig. 3**). By 36 hours, IFITM3 expression was largely restricted to the outer layers of the epidermis, indicating that local T_{RM} cell activation leads to a transient change in the skin transcriptome that is still visible in aging keratinocytes by the time newly formed keratinocytes have returned to steady state (**Fig. 3B**).

In most models of infection control by CD8$^+$ T cells, both the initial T cell activation and the final output signal (e.g., cytolysis) are dependent on recognition of cognate antigen. In contrast, the above-described tissue conditioning by T_{RM} cells requires antigen as input signal but generates an output signal—the up-regulation of genes involved in broad-spectrum defense—that does not rely on antigen recognition, a mechanism reminiscent of that of effector CD4$^+$ T cells (21). To test the potential relevance of this state of T_{RM} cell–induced "pathogen alert", we analyzed whether T_{RM} cell activation could lead to control of an antigenically unrelated pathogen *in vivo*. Skin resident OTI-GFP T_{RM} cells were activated by local injection of cognate peptide, and 9 hours later the same area was infected with antigenically unrelated HSV-1. At two time points after virus administration, progression of HSV-1 infections was scored microscopically (day 1) and macroscopically (day 3). As expected, disease progression in naïve mice was not influenced by $OVA_{257\text{-}264}$ peptide administration (**Fig. 4A**). In contrast, in mice harboring skin OTI-GFP T_{RM} cells, application of cognate $OVA_{257\text{-}264}$ peptide resulted in a strong reduction in HSV-1 disease severity relative to control conditions (**Fig. 4A**). Analysis of HSV-1–challenged skin tissue by staining with antibody to HSV showed that OTI-GFP T_{RM} cell activation resulted in a substantial reduction of both tissue necrosis and lateral spreading of herpetic lesions (**Fig. 4B**). In line with this, viral DNA levels were reduced in skin of mice harboring activated OTI-GFP T_{RM} cells at the time of infection (**Fig. 4C**, $P < 0.0001$). Taken together, these data demonstrate that the tissue conditioning that is induced by T_{RM} cell activation leads to enhanced pathogen control that is independent on the antigenic identity of this pathogen.

Three aspects of T_{RM} cell–mediated tissue conditioning are noteworthy. First, tissue conditioning is almost immediate. This property is likely to be of major relevance as, at least in case of HSV-2, early immune control is the major determinant of episode severity (14). Second, tissue conditioning forms an effective amplification system, in which activation of a rare cell type leads to a tissue wide response. Third, T_{RM} cell–mediated tissue conditioning

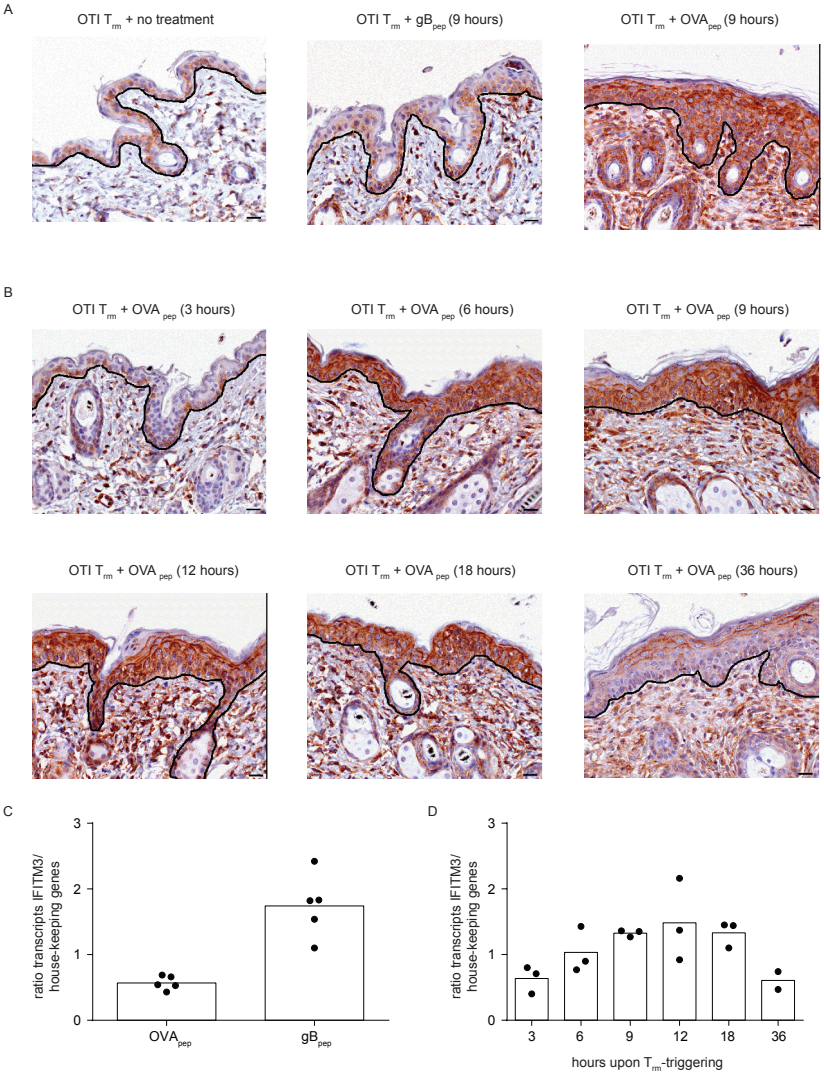

Figure 3 | Tissue conditioning by T_{RM} cells results in the induction of an antiviral state in large numbers of surrounding cells. (**A**) Immunohistochemical detection of IFITM3 in the skin of mice harboring OTI-GFP$^+$ T_{RM} cells, analyzed at steady state or 9 hours after treatment with either cognate $OVA_{257-264}$ or control $gB_{498-505}$ peptide (representative of three mice per group). (**B**) Immunohistochemical detection of IFITM3 in the skin of mice harboring OTI-GFP$^+$ T_{RM} cells at the indicated time points after treatment with $OVA_{257-264}$ peptide (representative of three mice per time point). The boundary between epidermis (top in all images) and dermis is highlighted by a black line. Scale bar, 20 μm. (**C** and **D**) Naive gBT-GFP$^+$ cells were transferred into recipients that were subsequently tattoo-vaccinated with DNA encoding TTFC-gB_{pep} to create a population of resident T_{RM} cells. Several weeks after tattooing, skin harboring T_{RM} cells was injected with either gB_{pep} or OVA_{pep} and processed for transcriptome analysis 9 hours later. (C) Ratio between IFITM3 counts and the median counts of 20 housekeeping genes. (D) The same analysis is depicted for samples in which skin harboring OTI T_{RM} cells was injected with OVA_{pep} and analyzed at the indicated time points.

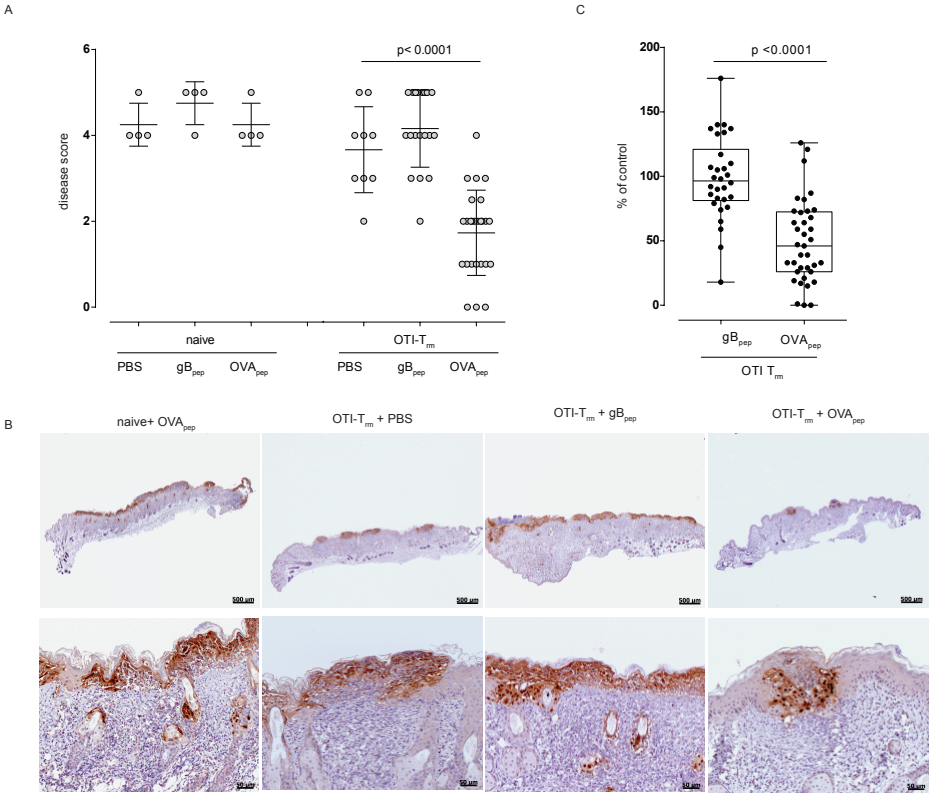

Figure 4 | CD8$^+$ T_{RM} cell triggering provides cross-protection against an antigenically unrelated pathogen. (**A**) Naïve mice or mice harboring OTI-GFP$^+$ T_{RM} cells (both hind legs) were injected locally with phosphate-buffered saline (PBS), cognate $OVA_{257-264}$ peptide, or control $gB_{498-505}$ peptide and locally infected with HSV-1 9 hours later. Sixty hours after infection, the extent of each infection was scored by visual inspection by an observer blinded to experimental group (all naïve groups: n = 2; OTI-T_{RM} + PBS: n = 5; T_{RM} + $gB_{498-505}$: n = 10; T_{RM} + $OVA_{257-264}$: n = 13; both legs analyzed separately). (**B**) Mice harboring OTI-GFP$^+$ T_{RM} cells (both hind legs) were injected locally with cognate $OVA_{257-264}$ peptide or control $gB_{498-505}$ peptide and were locally infected with HSV-1 9 hours later. After 60 hours, the amount of viral DNA in infected skin was measured. Data are representative of four independent experiments with at least five mice per group. To allow comparison between experiments, the amount of viral DNA in the OTI-TRM$^+$ $gB_{498-505}$ group was set to 100% for each experiment. (**C**) Immunohistochemical detection of HSV-1 infection in naïve mice that received a local injection with $OVA_{257-264}$ peptide (B) or mice harboring OTI-GFP$^+$ T_{RM} cells triggered with cognate $OVA_{257-264}$ peptide, control $gB_{498-505}$ peptide, or PBS (C). For each condition, two different magnifications of the same sample are shown. Data are representative of 2 (naïve group), 5 (T_{RM} + PBS), 10 (T_{RM} + $gB_{498-505}$), and 13 (T_{RM} + $OVA_{257-264}$) mice per group.

results in protection that is ultimately antigen independent: Although initial T_{RM} cell activation requires recognition of antigen, the genes that are up-regulated in response display activity toward a wide array of pathogens.

From a conceptual point of view, these data place T_{RM} cells as a bridge between the adaptive and innate immune system, in which the TCR in T_{RM} cells has a function similar to that of Toll-like receptors in innate immune cells. From a practical point of view, the fact that T_{RM} cell triggering leads to an output signal that no longer requires antigen recognition may also help counteract viral escape. Recently, strategies have been put forward to create T_{RM} cell populations at sites of potential pathogen entry (10, 22, 23). The current data not only help to provide a mechanistic explanation for the effects of such vaccines but also suggest that in case of pathogens that exist as quasispecies, protection may conceivably be provided not only against the vaccine-encoded sequence but also against viral variants that are transferred in parallel.

MATERIALS AND METHODS

Animals and reagents

gBT-GFP, OTI-GFP, OTI-GFP-Ifng$^{-/-}$, Ifngr1$^{-/-}$, C57Bl/6j mice and housing conditions have been described elsewhere (9). All mouse experiments were performed in accordance with institutional and national guidelines and were approved by the Experimental Animal Committee (DEC) of The Netherlands Cancer Institute.

Adoptive transfers, viral infection and peptide challenges

To induce skin T_{RM} populations, 5x10^5 naive CD8$^+$ T splenocytes from donor mice were adoptively transferred into recipient animals that were subsequently tattoo vaccinated three times (once every three days) in the hind legs with 2 µg DNA encoding the TTFC carrier protein plus the indicated peptide (9). Tattoo vaccination was carried out on the shaved flank of anaesthetized mice using a sterile disposable 11-needles bar mounted on a rotary tattoo device. Needle depth was adjusted to 0.5 mm with the needle bar oscillating at 100 Hz for a 60 s tattoo. Memory mice were considered as such at least three weeks after the final vaccination. To induce T_{RM} triggering, recipient mice harboring T_{RM} received either HSV-1 (~2.5x10^5 pfu in RPMI), peptide (3-4 µg in PBS/DMSO), or carrier by local microinjection (9). Alternatively, mice were injected intradermally with 3-4 µg peptide in 50 µl PBS/DMSO. At the indicated time points, animals were sacrificed and full-thickness skin of the treated area was collected by 6-mm punch biopsy.

Gene expression analysis and statistical analysis

After total RNA extraction (Trizol), library preparation was performed according to the manufacturer's protocol (Illumina). Transcriptomes were analyzed by applying the Bioconductor R package edgeR (24). For all analyses, biological replicates for each condition were included. Upstream Regulator Analysis (Ingenuity Pathway Analysis, Ingenuity® Systems, www.

ingenuity.com) was used to identify the upstream regulators that may be responsible for gene expression changes observed in experimental datasets. Housekeeping genes used for calibration of IFITM3 expression were Rpl22, Rps13, Ctdsp2, Atf4, Rpl30, Eif1, Anapc5, Gabarap, Rtn4, Ywhab, Set, Ube2d3, Cox4i1, Capzb, Ppp2ca, Gdi2, Arpc2, Canx, Fau and Naca. Figure bars indicate mean +/- SD. Differences between experimental conditions were analyzed by a two-sided Student's t-test.

Immunohistochemistry

For immunohistochemical analysis, 5µm thick semi-serial slices of formalin-fixed, paraffin-embedded tissue were stained with anti-IFITM3 (11714-1-AP, ProteinTech), anti-GFP (ab6556, Abcam), anti-F4/80 (MCA497, AbD Serotec), anti-Ly6g (551459, BD Biosciences), anti-CD45 (553076, BD Biosciences), anti-B220 (557390, BD Biosciences) anti-CD3 (RM-9107, Thermo Scientific), anti-Myeloperoxidase (A 0398, DakoCytomation), anti-Lysozyme (A 0099, DakoCytomation), rabbit polyclonal anti-HSVII (RB-1426-A1, Thermo Scientific), followed by HRP-labeled secondary antibody (DPVM-55-HRP, Immunologic) and DAB Chromogen detection (K3469, Dako). 3 Hematoxylin-eosin was used for counter staining. All stainings were performed after citrate buffer antigen retrieval.

Analysis of HSV-1 infection and viral DNA

One to three days after HSV-1 infection, the extent of herpetic lesions in living animals were scored microscopically (day one; size of the infection was quantified as the number of td-tomato positive pixels per image using ImageJ (9)) or macroscopically (day two and three; scoring range: 0 - no visible signs of infection; 1 -mild reddening and swelling; 3 -small scabs; 4 -small humid blisters; 5 - large humid blisters or open wounds) by observers blinded to experimental condition. The amount of viral DNA in infected skin was measured in 6mm punch biopsies enclosing the entire infected area (1 biopsy/infection). HSV titers were analyzed in triplicate for each sample, after DNA content normalization using the Artus HSV-1/2 TM PCR Kit (Qiagen), according to protocol.

Author contributions

S.A. and T.N.S. designed the study and wrote the manuscript; S.A., M.E.H. and F.E.D. designed and executed animal experiments; L.L.V. performed immunohistochemistry and J-Y.S. analyzed immunohistochemistry; M.A.H. designed and performed transcriptome analysis with conceptual insights provided by H.J.; J.B.H. participated in data interpretation and provided editorial comments.

Acknowledgements

We thank members of the Netherlands Cancer Institute Flow Cytometry, Digital Microscopy, Deep Sequencing Core, and Animal Pathology Facilities for technical support; R. van Mierlo

and M. Toebes for assistance; and members of the Schumacher laboratory for discussion. The data presented in this manuscript are tabulated in the main paper and in the supplementary materials. Expression data were deposited under Gene Expression Omnibus accession number GSE60599. This work was supported by The Netherlands Organization for Scientific Research grant 912.10.066 and European Research Council grant Life-his-T to T.N.S., and Dutch Cancer Society grant NKI-2008-4112 and The Netherlands Organization for Health Research and Development TOP grant 91213018 to H.J.

REFERENCES

1. S. Ariotti, J. B. Haanen, T. N. Schumacher, Adv. Immunol. 114, 203–216 (2012).
2. D. Masopust, V. Vezys, E. J. Wherry, D. L. Barber, R. Ahmed, J. Immunol. 176, 2079–2083 (2006).
3. T. Gebhardt et al., Nat. Immunol. 10, 524–530 (2009).
4. L. M. Wakim, A. Woodward-Davis, M. J. Bevan, Proc. Natl. Acad. Sci. U.S.A. 107, 17872–17879 (2010).
5. T. Gebhardt et al., Nature 477, 216–219 (2011).
6. M. Hofmann, H. Pircher, Proc. Natl. Acad. Sci. U.S.A. 108, 16741–16746 (2011).
7. X. Jiang et al., Nature 483, 227–231 (2012).
8. H. Shin, A. Iwasaki, Nature 491, 463–467 (2012).
9. S. Ariotti et al., Proc. Natl. Acad. Sci. U.S.A. 109, 19739–19744 (2012).
10. N. Çuburu et al., J. Clin. Invest. 122, 4606–4620 (2012).
11. M. Hofmann, A. Oschowitzer, S. R. Kurzhals, C. C. Krüger, H. Pircher, Eur. J. Immunol. 43, 2295–2304 (2013).
12. K. E. Mark et al., J. Infect. Dis. 198, 1141–1149 (2008).
13. J. T. Schiffer et al., Proc. Natl. Acad. Sci. U.S.A. 107, 18973–18978 (2010).
14. J. T. Schiffer, L. Corey, Nat. Med. 19, 280–290 (2013).
15. J. T. Schiffer et al., eLife 2, e00288 (2013).
16. B. Breart, F. Lemaître, S. Celli, P. Bousso, J. Clin. Invest. 118, 1390–1397 (2008).
17. J. M. Schenkel, K. A. Fraser, V. Vezys, D. Masopust, Nat. Immunol. 14, 509–513 (2013).
18. Materials and methods are available as supplementary materials on Science Online.
19. M. D. Young, M. J. Wakefield, G. K. Smyth, A. Oshlack, Genome Biol. 11, R14 (2010).
20. N. Yan, Z. J. Chen, Nat. Immunol. 13, 214–222 (2012).
21. A. J. Müleer et al., Immunity 37, 147-157 (2012).
22. S. G. Hansen et al., Nature 473, 523–527 (2011).
23. L. K. Mackay et al., Proc. Natl. Acad. Sci. U.S.A. 109, 7037–7042 (2012).
24. M. D. Robinson et al., Bioinformatics 26, 139-140 (2010).

SUPPLEMENTARY INFORMATION

Supplementary Table 1 | Genes differentially expressed upon challenge of T_{RM} skin. Columns indicate ensemble gene id. name and fold change for each replicate experiment (see also Fig. 1E). The right columns (in gray) indicate fold change for two independent experiments in which skin-gB T_{RM} were triggered with either HSV-1 or carrier. Genes were identified using the 3 step selection strategy described in Suppl. Fig. 3A.

		gBT T_{rm} + gB_{pep}		OTI T_{rm} + OVA_{pep}		gBT T_{rm} + HSV	
	Gene	exp1	exp2	exp3	exp4	exp5	exp6
ENSMUSG00000057191	AB124611	4.93	2.56	1.90	2.07	1.28	4.33
ENSMUSG00000075010	AW112010	4.33	3.92	6.97	8.07	0.07	0.40
ENSMUSG00000039699	Batf2	19.10	20.52	11.63	14.36	0.58	0.94
ENSMUSG00000029082	Bst1	6.45	3.39	2.69	1.61	5.38	7.02
ENSMUSG00000046718	Bst2	4.58	6.35	5.02	3.80	0.35	0.48
ENSMUSG00000035352	Ccl12	17.64	8.24	2.37	3.61	11.97	11.36
ENSMUSG00000035385	Ccl2	13.69	7.08	4.08	4.16	5.48	5.29
ENSMUSG00000025804	Ccr1	16.48	7.51	4.04	2.92	6.76	7.51
ENSMUSG00000052212	Cd177	18.06	13.54	3.10	5.34	16.73	26.83
ENSMUSG00000016496	Cd274	8.24	12.67	3.50	5.11	0.92	1.69
ENSMUSG00000000682	Cd52	2.37	1.99	1.85	2.96	0.69	0.41
ENSMUSG00000079293	Clec7a	7.29	14.82	6.05	7.67	0.27	1.72
ENSMUSG00000034855	Cxcl10	33.29	29.16	16.65	13.84	2.72	7.29
ENSMUSG00000029417	Cxcl9	34.57	42.25	56.10	46.38	4.67	6.25
ENSMUSG00000017830	Dhx58	7.84	6.15	4.33	2.99	0.50	2.07
ENSMUSG00000059089	Fcgr4	18.40	15.44	9.12	5.57	5.11	7.62
ENSMUSG00000028270	Gbp2	26.21	29.16	29.48	25.91	2.31	4.20
ENSMUSG00000028268	Gbp3	11.16	10.37	9.73	6.92	0.28	0.45
ENSMUSG00000079363	Gbp4	12.67	8.12	9.36	12.25	0.64	0.10
ENSMUSG00000040264	Gbp5	15.92	14.59	9.42	11.09	1.08	1.99
ENSMUSG00000079362	Gbp6	14.90	12.46	0.92	15.60	0.77	1.25
ENSMUSG00000040253	Gbp7	11.16	9.86	7.62	5.95	0.37	1.21
ENSMUSG00000029298	Gbp9	8.82	6.10	4.80	5.62	0.59	0.46
ENSMUSG00000082292	Gm12250	23.62	18.66	11.56	15.92	0.86	4.04
ENSMUSG00000029798	Herc6	8.24	8.88	8.70	2.69	0.52	0.94
ENSMUSG00000067212	H2-T23	1.44	4.16	2.04	2.62	0.19	0.03
ENSMUSG00000025877	Hk3	12.39	6.86	6.81	3.96	3.69	4.12
ENSMUSG00000010358	Ifi35	1.96	2.37	2.40	2.82	0.40	0.30
ENSMUSG00000028037	Ifi44	9.99	9.00	7.90	4.62	0.30	2.02
ENSMUSG00000078920	Ifi47	16.08	17.31	9.73	9.92	1.02	1.82
ENSMUSG00000034459	Ifit1	12.32	8.94	9.61	4.45	0.49	3.06
ENSMUSG00000074896	Ifit3	6.71	3.65	2.82	2.69	0.03	0.35
ENSMUSG00000025491	Ifitm1	7.18	1.64	3.46	2.53	4.67	4.80
ENSMUSG00000025492	Ifitm3	2.82	3.42	1.93	2.46	6.30	3.53
ENSMUSG00000078853	Igtp	22.94	18.06	14.59	15.13	1.42	2.13
ENSMUSG00000054072	Iigp1	27.14	21.53	18.49	16.89	2.13	1.82
ENSMUSG00000031289	Il13ra2	2.04	4.45	3.96	1.88	4.41	1.61
ENSMUSG00000070427	Il18bp	4.80	2.96	6.40	5.43	0.32	1.25
ENSMUSG00000026068	Il18rap	7.45	10.89	3.24	2.62	5.29	2.99
ENSMUSG00000018899	Irf1	9.30	12.18	4.45	8.41	1.23	0.81
ENSMUSG00000025498	Irf7	6.35	7.62	3.24	3.20	0.26	1.08
ENSMUSG00000046879	Irgm1	12.39	12.18	6.50	8.18	0.96	1.80
ENSMUSG00000069874	Irgm2	11.42	7.67	4.80	6.71	0.83	2.16
ENSMUSG00000035692	Isg15	13.32	16.40	11.42	9.73	0.41	3.28
ENSMUSG00000026822	Lcn2	6.00	1.82	4.45	3.06	10.96	16.73

		gBT T_{rm} + gB_{pep}		OTI T_{rm} + OVA_{pep}		gBT T_{rm} + HSV	
	Gene	exp1	exp2	exp3	exp4	exp5	exp6
ENSMUSG00000062593	Lilrb4	10.69	4.75	3.13	1.82	5.90	4.04
ENSMUSG00000075602	Ly6a	2.50	2.79	1.72	1.44	0.45	0.38
ENSMUSG00000012519	Mlkl	8.01	6.66	6.60	4.28	1.69	3.31
ENSMUSG00000000386	Mx1	11.29	11.90	5.24	2.37	-0.04	-0.07
ENSMUSG00000026946	Nmi	5.66	5.38	6.40	5.62	0.49	0.79
ENSMUSG00000020826	Nos2	21.53	10.37	7.90	7.56	15.05	21.53
ENSMUSG00000052776	Oas1a	8.18	9.55	6.55	4.67	0.74	1.82
ENSMUSG00000066861	Oas1g	7.34	11.42	8.82	3.20	0.56	1.12
ENSMUSG00000029561	Oasl2	12.67	15.52	8.24	3.96	0.42	1.04
ENSMUSG00000049401	Ogfr	1.85	1.61	1.54	1.64	0.12	0.42
ENSMUSG00000063268	Parp10	3.35	4.93	2.46	3.31	0.49	0.45
ENSMUSG00000038507	Parp12	5.90	6.50	4.54	4.08	0.49	1.46
ENSMUSG00000034422	Parp14	7.62	9.24	3.39	2.16	0.76	1.72
ENSMUSG00000022906	Parp9	5.43	5.71	4.41	3.72	0.59	1.04
ENSMUSG00000068245	Phf11d	6.30	7.24	3.46	3.76	0.61	1.44
ENSMUSG00000029322	Plac8	6.45	2.62	4.97	4.62	3.28	5.34
ENSMUSG00000031897	Psmb10	5.20	5.57	6.97	6.45	0.34	0.28
ENSMUSG00000024338	Psmb8	4.41	7.02	6.25	6.05	0.38	0.10
ENSMUSG00000029204	Rhoh	5.38	8.41	2.28	1.82	2.89	0.56
ENSMUSG00000020641	Rsad2	13.32	5.38	6.50	1.77	1.39	5.62
ENSMUSG00000033355	Rtp4	9.55	7.45	5.52	4.24	0.50	1.80
ENSMUSG00000027639	Samhd1	5.81	7.67	4.45	4.41	0.50	1.04
ENSMUSG00000053318	Slamf8	13.91	9.61	9.80	7.90	1.21	0.28
ENSMUSG00000024737	Slc15a3	8.64	4.49	1.82	1.55	4.80	5.90
ENSMUSG00000078763	Slfn1	19.62	9.24	5.34	2.46	3.35	3.76
ENSMUSG00000072620	Slfn2	7.34	4.58	2.89	2.66	2.62	3.57
ENSMUSG00000031662	Snx20	4.84	4.33	2.82	2.82	1.42	2.16
ENSMUSG00000038037	Socs1	7.62	7.08	2.19	8.07	2.34	5.43
ENSMUSG00000070034	Sp110	5.34	6.55	3.03	1.90	0.18	0.79
ENSMUSG00000020077	Srgn	10.24	6.00	3.39	3.03	7.08	6.45
ENSMUSG00000026104	Stat1	6.97	7.02	4.54	4.20	0.26	0.77
ENSMUSG00000022902	Stfa2	6.05	1.96	9.79	7.78	3.06	7.45
ENSMUSG00000054905	Stfa3	2.10	1.64	7.62	7.02	2.92	3.20
ENSMUSG00000037321	Tap1	2.31	5.20	2.34	4.08	0.12	0.08
ENSMUSG00000024339	Tap2	2.66	5.29	3.69	3.61	0.14	0.08
ENSMUSG00000024308	Tapbp	1.99	4.93	3.13	3.65	0.07	0.20
ENSMUSG00000053338	Tarm1	16.89	10.05	6.25	7.34	7.24	8.24
ENSMUSG00000029553	Tfec	6.15	3.28	4.00	3.20	3.46	7.08
ENSMUSG00000032596	Uba7	4.41	6.30	3.06	2.56	0.32	0.35
ENSMUSG00000027078	Ube2l6	4.75	7.67	4.58	5.57	0.23	0.74
ENSMUSG00000030107	Usp18	5.38	8.41	2.66	2.25	0.05	1.30
ENSMUSG00000069792	Wfdc17	4.54	3.35	2.31	3.03	4.67	5.24
ENSMUSG00000040483	Xaf1	6.55	9.30	5.66	3.96	0.66	0.64
ENSMUSG00000027514	Zbp1	14.75	10.11	7.51	5.34	0.55	2.25

Supplementary Table 2 | Top 50 Gene Ontology terms in data set 1-4 as identified by GOSeq.

category	Description	exp. 1	exp. 2	exp. 3	exp. 4
GO:0006952	defense response	1.66E-73	2.37E-50	1.45E-30	1.76E-27
GO:0002376	immune system process	1.23E-73	2.16E-44	5.70E-38	3.51E-26
GO:0006955	immune response	3.74E-66	1.33E-42	1.72E-33	1.98E-22
GO:0051707	response to other organism	1.28E-55	1.28E-38	3.47E-32	1.59E-24
GO:0009607	response to biotic stimulus	6.47E-56	9.13E-38	8.52E-31	2.12E-23
GO:0009611	response to wounding	2.36E-28	7.94E-35	2.54E-06	3.51E-07
GO:0051704	multi-organism process	1.84E-45	2.74E-30	2.37E-28	1.88E-19
GO:0045087	innate immune response	5.78E-42	5.40E-30	7.71E-26	1.38E-20
GO:0006954	inflammatory response	6.56E-34	1.58E-28	4.87E-07	2.66E-08
GO:0002252	immune effector process	2.97E-39	7.49E-27	1.75E-15	5.08E-12
GO:0042221	response to chemical stimulus	1.28E-36	1.11E-26	3.29E-16	2.77E-16
GO:0034097	response to cytokine stimulus	1.87E-33	1.93E-26	2.04E-21	1.50E-16
GO:0050896	response to stimulus	8.83E-41	3.87E-25	8.65E-13	2.35E-12
GO:0071345	cellular response to cytokine stimulus	5.05E-31	2.77E-24	2.21E-22	3.25E-18
GO:0002682	regulation of immune system process	6.50E-34	2.91E-23	1.22E-11	1.11E-06
GO:0010033	response to organic substance	1.07E-32	4.97E-23	1.66E-14	1.54E-16
GO:0001817	regulation of cytokine production	2.36E-26	1.06E-22	8.85E-11	3.39E-07
GO:0001816	cytokine production	6.04E-30	6.33E-22	1.11E-10	4.36E-07
GO:0009617	response to bacterium	7.93E-28	8.39E-22	1.68E-14	2.97E-13
GO:0050900	leukocyte migration	7.21E-23	9.99E-22	2.06E-08	2.02E-12
GO:0002684	positive regulation of immune system process	1.72E-31	2.26E-21	1.43E-12	2.24E-06
GO:0009605	response to external stimulus	1.62E-21	2.74E-21	3.40E-04	1.32E-07
GO:0070887	cellular response to chemical stimulus	5.56E-24	4.33E-21	8.44E-14	1.69E-12
GO:0032501	multicellular organismal process	1.95E-15	6.64E-21	2.82E-05	5.94E-08
GO:0051239	regulation of multicellular organismal process	1.33E-20	9.34E-21	3.94E-07	2.71E-07
GO:0031347	regulation of defense response	2.55E-27	9.81E-21	2.42E-08	2.18E-09
GO:0042742	defense response to bacterium	3.64E-20	9.90E-20	2.65E-12	3.94E-10
GO:0006935	chemotaxis	1.37E-14	1.23E-18	6.56E-07	4.25E-08
GO:0006950	response to stress	1.89E-31	1.46E-18	1.17E-16	5.70E-12
GO:0042330	taxis	1.55E-14	1.54E-18	6.76E-07	4.54E-08
GO:0009615	response to virus	6.33E-30	6.77E-18	4.17E-19	2.29E-11
GO:0032101	regulation of response to external stimulus	6.03E-17	1.05E-17	4.62E-04	3.99E-06
GO:0030595	leukocyte chemotaxis	8.13E-21	1.60E-17	8.24E-10	6.86E-13
GO:0031349	positive regulation of defense response	2.60E-17	1.26E-16	1.17E-06	1.11E-07
GO:0048584	positive regulation of response to stimulus	9.05E-22	2.63E-16	2.18E-09	3.13E-05
GO:0060326	cell chemotaxis	7.72E-19	4.12E-16	1.49E-08	4.20E-11
GO:0002237	response to molecule of bacterial origin	1.81E-20	6.33E-15	3.29E-09	2.01E-07
GO:0001819	positive regulation of cytokine production	2.86E-20	1.51E-14	1.01E-09	1.95E-07
GO:0002697	regulation of immune effector process	5.52E-24	1.60E-14	5.88E-11	3.55E-06
GO:0071310	cellular response to organic substance	3.03E-16	1.79E-14	1.67E-13	1.48E-10
GO:0080134	regulation of response to stress	6.94E-20	4.56E-14	4.11E-06	1.42E-05
GO:0035456	response to interferon-beta	1.42E-13	1.88E-13	8.88E-14	2.97E-14
GO:0030593	neutrophil chemotaxis	2.88E-14	3.63E-13	4.38E-05	3.59E-09
GO:0050795	regulation of behavior	8.11E-07	6.02E-13	3.14E-06	3.94E-07
GO:0002685	regulation of leukocyte migration	5.99E-09	8.95E-13	9.50E-06	3.62E-07
GO:0050663	cytokine secretion	3.07E-15	9.40E-13	5.65E-06	3.32E-06
GO:0032103	positive regulation of response to external stimulus	3.67E-11	1.04E-12	1.60E-07	1.84E-08
GO:0035458	cellular response to interferon-beta	3.77E-14	1.30E-12	3.29E-14	1.10E-14
GO:0050707	regulation of cytokine secretion	2.50E-14	1.30E-12	3.05E-04	3.47E-06
GO:0051240	positive regulation of multicellular organismal process	1.14E-16	1.66E-12	8.85E-08	2.04E-07

exp. 1	Fold Change	activation state	Bias-corrected z-score	p value	Target molecules in data set
IFNγ	14.32	activated	7.779	1.65E-70	144/144
TNF	6.82	activated	6.256	2.14E-32	88/88
IL1B	24.17	activated	5.468	1.29E-33	68/68
TNF	5.72	activated	4.440	6.23E-47	73/73
TNFSF12	-	activated	3.970	4.83E-29	37/37

exp. 2	Fold Change	activation state	Bias-corrected z-score	p value	Target molecules in data set
IFNγ	45.68	activated	4.266	2.73E-73	85/85
IFNB1	-	activated	3.118	6.12E-52	49/49
TNF	4.83	activated	2.965	6.46E-12	26/26
IL1B	5.19	activated	2.651	1.55E-13	22/22
TNFSF12	-	activated	2.482	7.82E-19	18/18

exp. 3	Fold Change	activation state	Bias-corrected z-score	p value	Target molecules in data set
IFNγ	6.24	activated	9.152	4.64E-49	106/106
TNF	0.89	activated	6.863	8.25E-19	59/59
IFNB1	-	activated	6.130	5.90E-33	54/54
IL1B	2.94	activated	5.726	2.91E-16	41/41
TNFSF12	-	activated	5.162	2.06E-22	29/29

exp. 4	Fold Change	activation state	Bias-corrected z-score	p value	Target molecules in data set
IFNγ	42.02	activated	5.021	7.34E-56	90/90
IFNB1	-	activated	3.927	1.18E-41	51/51
IL1B	1.57	activated	3.321	2.53E-18	34/34
TNF	0.39	activated	3.208	6.56E-20	46/46
TNFSF12	-	activated	2.759	4.97E-22	24/24

Supplementary Table 3 | Analysis of upstream regulators. Upstream regulator analysis was used to identify the most likely regulators responsible for the gene expression changes observed upon triggering of skin-T_{RM} with cognate peptide. Columns indicate: name of the regulating cytokine; fold change of

regulator cytokine in experimental dataset; bias-corrected z-score (indicates the significance of the observed predictions, considered significant when z> ±2); p value (indicates whether there is a statistically significant overlap between the data set genes and the genes that are regulated by the transcriptional regulator); target molecules in the data set (the fraction of relevant genes in the data set that behave in accordance with predicted regulator status).

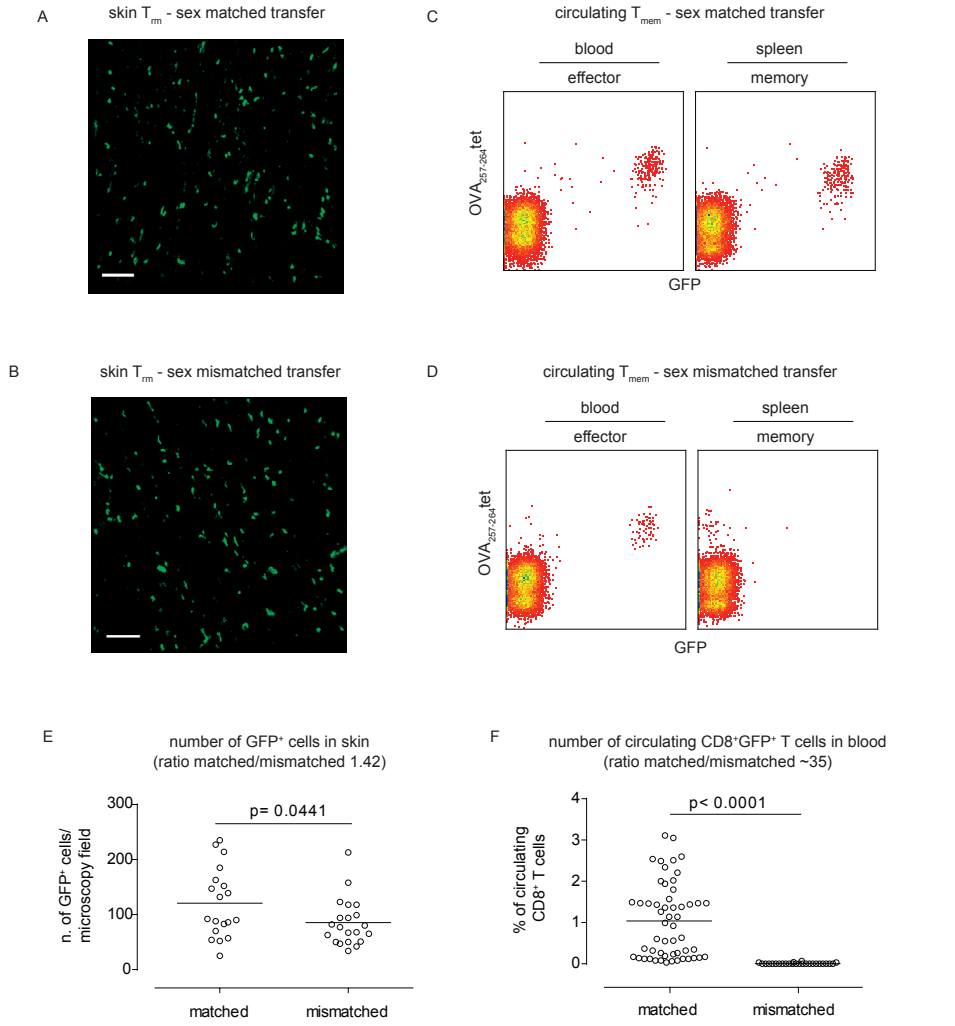

Supplementary Figure 1 | Frequency of resident and circulating memory CD8⁺ T cells in sex-matched and mismatched recipients. A-D) Naive OTI-GFP⁺ T cells of female (sex-matched, A, C) or male (sex-mismatched, B, D) origin were transferred into female recipients that were subsequently tattoo-vaccinated with DNA encoding TTFC-OVA_{pep}, in order to create a population of resident T_{RM}. Several weeks after tattooing, the skin harboring T_{RM} was imaged by confocal microscopy and blood was collected to quantify the percentage of circulating memory T cells of donor origin. Snapshots are representative of at least five mice from different experiments, flow cytometry plots are representative of 26 mice (quantification in panels E, F). **E**) Quantification of the numbers of OTI-GFP⁺ cells detected in non-overlapping T_{RM}-harboring skin areas of mice from different experiments. Similar results were obtained when gBT T cells were utilized. **F**) The amount of circulating memory OTI-GFP⁺ or gBT-GFP⁺ T cells in blood of mice that received sex-matched or sex-mismatched donor cells (matched: n=54 from 4 different experiments; sex-mismatched n=26 from 3 different experiments). Note that in spite of the variability in frequencies, circulating memory CD8⁺ T cells were always detected in blood of sex-matched recipients, while in only one case out of 26, a small population (0.067%) was detected upon sex-mismatched adoptive transfer.

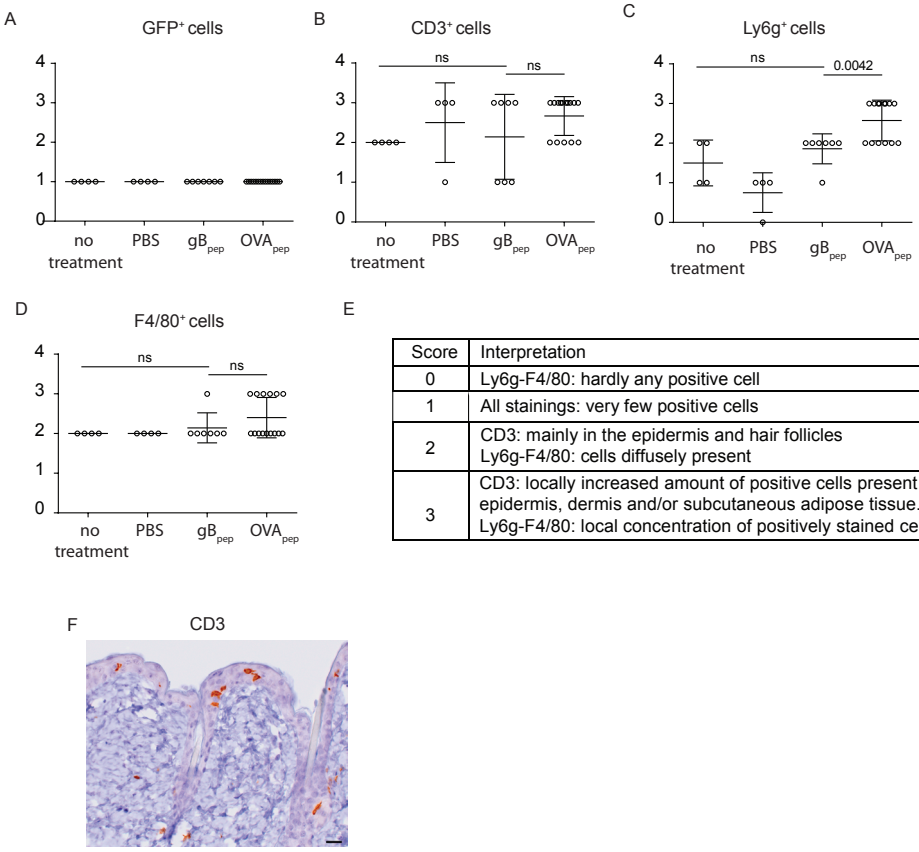

E

Score	Interpretation
0	Ly6g-F4/80: hardly any positive cell
1	All stainings: very few positive cells
2	CD3: mainly in the epidermis and hair follicles Ly6g-F4/80: cells diffusely present
3	CD3: locally increased amount of positive cells present in epidermis, dermis and/or subcutaneous adipose tissue. Ly6g-F4/80: local concentration of positively stained cells

Supplementary Figure 2 | Frequency of various cell types in challenged T_{RM}-harboring skin. **A-D**) Naive OTI-GFP$^+$ T cells were transferred into recipients that were subsequently tattoo-vaccinated with DNA encoding TTFC-OVA_{pep} in order to create a population of resident T_{RM}. Several weeks after tattooing, full-thickness skin was treated locally with gB_{pep}, OVA_{pep}, or PBS, or left untreated. After 9 hrs, skin was collected and processed for the detection of GFP$^+$ cells (as a surrogate marker for adoptively transferred CD8$^+$ T cells), CD3$^+$ cells, Ly6g$^+$ cells (neutrophils) and F4/80$^+$ cells (macrophages) by immunohistochemistry. Results are derived from a minimum of four mice from at least two independent experiments. Several non-consecutive slices of each sample were analyzed by an observer blinded to experimental condition and scored according to the scale in **E**). **F**) Representative result of anti-CD3 immunohistochemistry staining (positive cells are brown; bar = 20 µm).

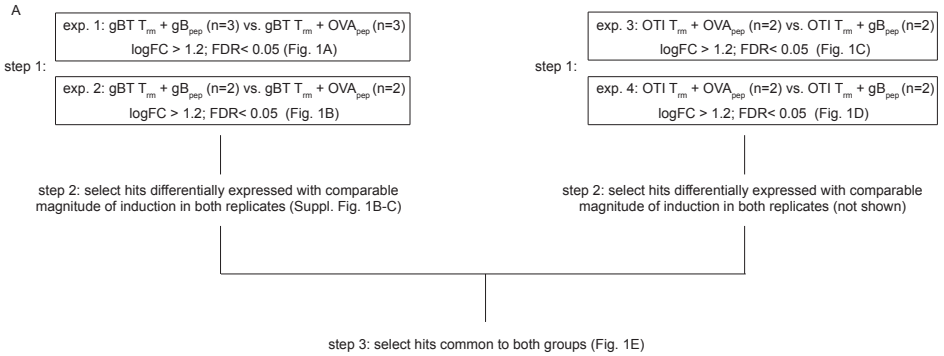

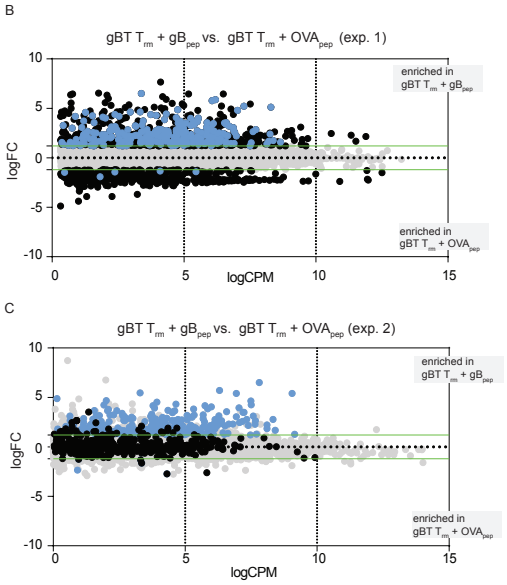

Supplementary Figure 3 | Selection strategy for identification of genes differentially expressed upon triggering of skin-resident T_{RM}. A) Mice harboring either gBT or OTI skin-T_{RM} were injected locally with either gB_{pep} or OVA_{pep}. Nine hours later, animals were sacrificed and skin collected for transcriptome analysis. Step 1: transcriptome analysis was performed to identify differentially expressed genes in each replicate (threshold: logFC>±1.2, FDR<0.05). Step 2: in order to eliminate noise due to sample variability, only those genes that were differentially expressed in an independent data set using T_{RM} with the same specificity, and that displayed a comparable magnitude of induction (difference in the magnitude of induction <1.5) were retained. Step 3: Data sets obtained using gBT or OTI skin-T_{RM} were combined and those genes that were differentially expressed in both experimental systems were retained. **B-C**) Transcriptome analysis of skin harboring gB T_{RM} triggered with either gB_{pep} or OVA_{pep}. Genes that are differentially expressed in both data sets are depicted in blue, genes that are differentially expressed in exp. 1 but not exp. 2 are depicted in black in both panels. All other genes are depicted in gray. The same analysis was performed for OTI T_{RM} data sets (not shown).

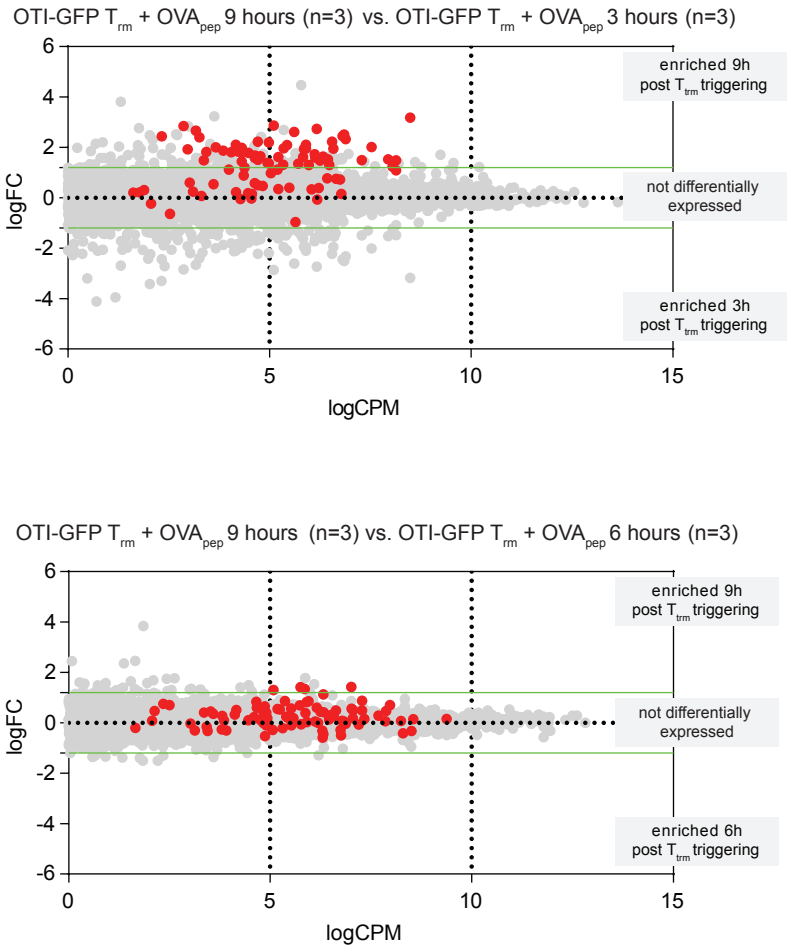

Supplementary Figure 4 | Differential expression of hit genes at different time points after T_{RM} triggering. Naive OTI-GFP$^+$ T cells were transferred into recipients that were subsequently tattoo-vaccinated with DNA encoding TTFC-OVA_{pep} in order to create a population of resident T_{RM}. Several weeks after tattooing, skin harboring T_{RM} was injected with OVA_{pep} or gB_{pep}, and 3 hrs, 6 hrs, or 9 hrs later processed for transcriptome analysis. Genes listed in Table 1 are depicted in red. All transcripts not part of the identified gene set are depicted in gray.

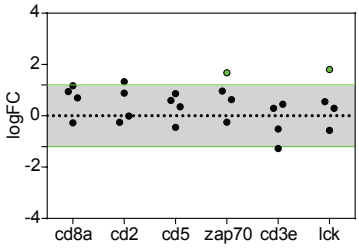

Supplementary Figure 5 | T cell specific gene expression upon T_{RM} activation. LogFC of various T-cell specific transcripts is indicated for four different comparisons. Black dots indicate genes that are not differentially expressed, green dots genes that are differentially expressed. Note that there is no significant increase in T-cell specific transcripts early upon T_{RM} triggering.